Electrocatalysis (2013) 4:92–100
DOI 10.1007/s12678-013-0124-7

Electrochemical Properties of Oxo–Manganese Complex Biomimicking Enzyme Active Sites and Its Electrocatalytic Application for Dopamine Determination

C. S. Martin · M. F. S. Teixeira

Published online: 15 January 2013

Abstract This work describes the characterization of the $[Mn_2^{IV,IV}O_2(terpy)_2(H_2O)_2]^{4+}$ complex in aqueous solution by UV–vis spectrophotometry, cyclic voltammetry, and linear sweep voltammetry with a rotating disk electrode. The pH effect, potential scan rate, effect of perfluorosulfonate polymer, and anion of supporting electrode on the electrochemical behavior of the modified electrode for better performance were investigated. The potential peak of the modified electrode was linearly dependent upon the ratio [ionic charge]/[ionic radius]. The modified electrode exerted an electrocatalytic effect on dopamine oxidation in aqueous solution with a decrease in the overpotential compared with the unmodified glassy carbon electrode. This way, the modified electrode showed an enzymatic biomimicking behavior. Tafel plot analyses were used to elucidate the kinetics and mechanism of dopamine oxidation.

Keywords Oxo–manganese complex · Electrochemical behavior · Enzymatic biomimicking · Electrocatalysis · Dopamine

Introduction

Polynuclear complexes of oxo–manganese ([(ligand)Mn(IV)-O_2-Mn(IV)(ligand)]$^{3+}$) show processes of multi-step electron transfer which result in good stability for high states of oxidation and capacity of charge exchange between manganese ions [1]. The complex $[Mn_2^{IV,IV}O_2(terpy)_2(H_2O)_2]^{4+}$ (terpy = 2,2′:6,2″–terpyridine) is a dimer capable of promoting the catalytic reaction of oxidation of the molecule H_2O by oxidizing agents/oxygen atom donors such as peroxymonosulfate (HSO_5^-) and hypochlorite in solution [2]. Binuclear complexes of manganese have received substantial attention through the study of analogous and synthetic models, with the aim of biomimicking the active site of various enzymes in homogeneous as well as heterogeneous catalysis. The strategy of utilizing different ligands in the preparation of the complex has helped in the understanding of the structure–function relation of the manganese ion in various modelings of metalloproteins and elucidation of the role this metal ion in enzymes [3]. This importance in biology has generated various complexes, which are currently applied as catalysts and electrocatalysts for the oxidation of alcohols [4, 5], organic compounds [6–9], and water [10, 11].

The synthesis of binuclear complexes of manganese containing terpyridine (tridentate ligand) and a molecule of aqua at each end is of great interest in the area of catalysis due to its stability in aqueous media. The stability of the $[Mn_2^{IV,IV}O_2(terpy)_2(H_2O)_2]^{4+}$ complex in aqueous solutions was evaluated by the persistence of the red color of the solution and by the lack of any change in spectral absorption during its storage. In contrast to the complexes di-μ-oxo of bpy and phen, the $[Mn_2^{IV,IV}O_2(terpy)_2(H_2O)_2]^{4+}$ complex is insoluble in organic solvents such as CH_3CN and CH_2Cl_2, but soluble in non-buffered aqueous solution [12–14].

This article describes the electrochemical characterization of the complex $[Mn_2^{IV,IV}O_2(terpy)_2(H_2O)_2]^{4+}$ in aqueous solution by cyclic voltammetry and linear voltammetry with a rotating disk electrode, and the immobilization of the complex on a glassy carbon electrode covered with the

Electronic supplementary material The online version of this article (doi:10.1007/s12678-013-0124-7) contains supplementary material, which is available to authorized users.

C. S. Martin · M. F. S. Teixeira (✉)
Department of Physics, Chemistry and Biology—Faculty of Science and Technology, University of State of Sao Paulo (UNESP), Rua Roberto Simonsen, 305,
CEP 19060-900, Presidente Prudente, SP, Brazil
e-mail: funcao@fct.unesp.br

polymer polytetrafluoroethylene sulfonate (ionic polymer perfluorosulfonate—Nafion®). In addition, the kinetic parameters were determined to evaluate the performance of the modified electrode as a mediator of electrons for catalytic oxidation of dopamine.

Experimental

Reagents and Solution

The NaCl, $NaNO_3$, $NaClO_4$, and Na_2SO_4 of high purity were used as support electrolyte (solution at 0.5 $mol L^{-1}$). The pH study was performed in 0.1 $mol L^{-1}$ acetate buffer solution in the range of 2.0 to 6.0. The pH of these solutions was adjusted using concentrated HCl and NaOH. The Nafion® (5 % *v*/*v*—Aldrich) solution was used as ion-exchange polymers on electrode surface. The variation of Nafion® concentration was obtained by dilution in ethanol of high purity.

$[Mn_2^{IV,IV}O_2(terpy)_2(H_2O)_2](NO_3)_4{\cdot}6H_2O$ Synthesis

The $[Mn_2^{IV,IV}O_2(terpy)_2(H_2O)_2](NO_3)_4{\cdot}6H_2O$ complex was synthesized according to adaptations of the literature procedure [2]. 2,2′:6,2"–terpyridine (Fluka; 0.72 mmol) was dissolved in acetone (Synth), in which $MnNO_3{\cdot}4H_2O$ (Aldrich; 0.48 mmol) in H_2O was added. After all reactants were dissolved, the yellow mixture was stirred in an ice bath for 15 min. Then the $KMnO_4$ (Aldrich; 1.3 mmol) in water was added dropwise to the mixture, which turned deep green in about 15 min. The mixture was kept in stirring for 30 min, was cooled after at 5 °C for 24 h. The solids were carefully separated and washed with several drops water. The final product was left in desiccators for complete evaporation of the solvent.

Characterization

The complex was characterized by UV–vis spectroscopy, cyclic voltammetry, and linear sweep voltammetry with a rotating disk electrode (RDE) in 0.5 $mol L^{-1}$ $NaNO_3$ solution as support electrolyte containing 1.0 $mmol L^{-1}$ of the complex. The absorbance measurements were performed in an UV–vis Spectrophotometer (UV-1650PC—SHIMADZU) in spectrum range of 400 to 900 nm. All voltammetric measurements were carried out in a 25-mL thermostatic glass cell at 25 °C containing three electrodes: a glassy carbon electrode as the working electrode (surface area of 0.071 cm^2), a saturated calomel electrode (SCE) as the reference electrode, and a platinum auxiliary electrode. All electrodes were connected to μAutolab Type III potentiostat/galvanostat (Eco Chimie—Netherlands) controlled by a personal computer. Prior to use, the working electrode was polished with an aqueous solution suspension of 0.05 μm alumina slurry, washed with ethanol, and then rinsed with water and ethanol. The cyclic voltammograms were obtained from 0.25 to 1.2 V vs. SCE potential range at 25 $mV s^{-1}$. The polarization curves (RDE—study) were obtained from 0 to 1.0 V vs. SCE potential range and 100 to 5,000 rpm (rotation rate) at 25 $mV s^{-1}$. The electrochemical behavior of the electrode modified with oxo–manganese–terpyridine complex immobilized in Nafion® was instigated by cyclic voltammetry.

Modified Electrode Construction

The electrode modified was obtained by addition of an aliquot of the Nafion® by casting method, and then kept in dissector for 8 h to solvent evaporation, forming a polymeric film on electrode surface. After, the immobilization of the complex was realized on the polymeric ionic exchange, adding 50 μL of the 1.0 $mmol L^{-1}$ $[Mn_2^{IV,IV}O_2(terpy)_2(H_2O)_2]^{4+}$ solution (complex dissolved in 0.5 $mol L^{-1}$ $NaNO_3$ solution). The modified electrode (GC-Nafion/MnTerpy) was washed with deionized water and subjected to potential scans in 0.5 $mol L^{-1}$ $NaNO_3$ (pH 4.7). The variation of Nafion® concentration (1–5 % *v*/*v*) and amount of aliquot used (3–9 μL) onto electrode surface were investigated.

Dopamine Electrocatalytic Oxidation

Electrocatalytic study of the modified electrode for dopamine oxidation was realized by cyclic voltammetry. The cyclic voltammograms were obtained from 0.45 to 1.2 V vs. SCE potential range at 25 $mV s^{-1}$ with adding of the aliquot of dopamine solution (0.025 to 0.556 $mmol L^{-1}$). The performance of modified electrode for dopamine oxidation was evaluated by the decrease of overpotential of the dopamine oxidation and increase of electrocatalytic current.

Results and Discussion

Characterization by UV–Vis Spectrophotometry

The absorption spectrum obtained in the range of 400 to 900 nm displayed two absorption bands, as shown in Fig. 1. The band at 553 nm can be ascribed to the band of the *d*–*d* transition of the metal, while the band at 642 nm is due to the charge transfer from the metal to the oxygen ligand of the complex, where this is in agreement with reports in the literature [2, 4, 15–17].

The complexes of the di-μ-oxo type can show three types of electron transitions [15]: (1) *d*–*d* transition of the metal; (2) *d*–*d* transition between the metal centers in the same

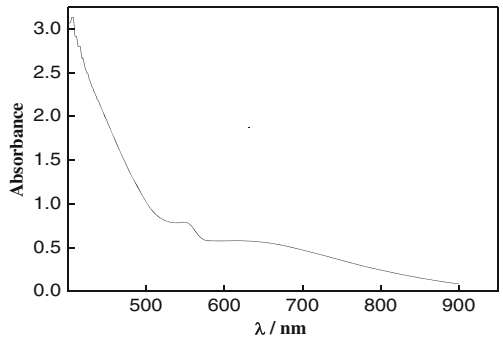

Fig. 1 UV–vis spectrum for 1.0 mmolL^{-1} of the $[Mn_2^{IV,IV}O_2(terpy)_2(H_2O)_2]^{4+}$ complex in 0.5 molL^{-1} $NaNO_3$ solution (pH = 4.7)

complex, and (3) transition between metal and ligand. The Mn^{IV} ion displays a d^3 electron distribution, and thus, *d–d* electronic transition occurs in the orbitals $t_{2g}{}^3 \rightarrow t_{2g}{}^2\ e_g{}^1$, where this mechanism is dominant in high-energy regions and involves the transfer of a single electron [15]. The Mn^{IV}–oxo charge transition occurs preferentially in the *dxy* orbital (in the same plane as the Mn–oxo bond) rather than the dz^2 transition, which is situated perpendicular to the Mn–oxo plane. Also, the transitions of the *dxz* and *dyz* orbitals show lower energy (less charge transfer) because they are perpendicular to the Mn–oxo plane. Therefore, it is concluded that the transition of greater energy is ascribed to charge transfer between the *dxy* orbital of the Mn^{IV}–oxo bond. In this system, superposition of the orbitals can occur at t_{2g}, causing a displacement to regions of higher energy. In the Mn^{III} ion (system d^4), there is a tetragonal distortion, which stabilizes the complex distributing the electrons to the occupied and empty orbitals t_{2g} and e_g, respectively. The *d-d* transition occurs in the octahedrial structure with electron transfer at $t_{2g}{}^3\ e_g{}^1 \rightarrow t_g{}^2\ e_g{}^2$ which involves only the passage of a single electron. Thus, this structure can undergo a Jahn Teller effect in the *z*-axis. In regions of low energy the electron transfer $dx^2y^2 \rightarrow dxy$ can occur, involving orbital with orientations in the equatorial plane (Mn–oxo plane). The *d-d* electron transfer of the Mn^{III} ion occurs between the *dxz* and *dxy* orbitals (*dxz* → *dxy)*. Because they are degenerate orbitals (t_{2g}), electron transfer occurs at lower energies than that observed in Mn^{IV}, which is known as the Jahn Teller effect. The Jahn Teller effect reflects the energy of stabilization of the electron in the orbital dz^2 of the Mn^{III} ion, but with influence of the ligand field present, the promotion of an electron, $dz^2 \rightarrow dxy$, can occur, relating the energies of axial bonds (perpendicular to the Mn–oxo bond) [15]. The transition $Mn^{III} \rightarrow Mn^{IV}$ can occur by polarization of low energy and will be determined by the redox potentials, where the charge effect of the Mn^{III} ion is dominant over the Jahn Teller effect [15, 18] in determining the ionization potential of the dz^2 orbital.

Electrochemical Characterization by Cyclic Voltammetry

The cyclic voltammogram (see Fig. 2) obtained in the potential range of 0.2 to 1.2 V vs. SCE in 0.5 molL^{-1} $NaNO_3$ shows a quasi-reversible process with $E_{1/2}$= 0.75 V vs. SCE ($E_{1/2} = (E_{pa} + E_{pc})/2$). The voltammogram obtained shows a redox process ascribed to the pair $Mn^{IV}Mn^{IV}/Mn^{III}Mn^{IV}$, characteristic of a multi-step process of electron transfer. In the literature, some voltammograms indicate the formation of binuclear species of the $Mn^{III}Mn^{III}$ type, conferring irreversibility to the system, characteristic of these complexes due to the Jahn Teller effect [1, 19]. Electrochemical reduction of $[Mn_2^{IV,IV}O_2(terpy)_2(H_2O)_2]^{4+}$ leads to the aggregation of two $[Mn_2^{III,IV}O_2(terpy)_2(H_2O)_2]^{3+}$ species forming the species $[Mn_4{}^{IV}O_5(terpy)_4(H_2O)_2]^{6+}$ with the addition of a new μ-oxo-bridged and oxidation of Mn^{III} ions to Mn^{IV}, as shown in Eq. 1:

$$2\left[Mn_2^{III,IV}O_2(terpy)_2(H_2O)_2\right]^{3+} + \left[Mn_2^{IV}O_2(terpy)_2(H_2O)_2\right]^{4+} + 2H^+ \rightleftarrows \left[Mn_4^{IV}O_5(terpy)_4(H_2O)_2\right]^{6+} + 2\left[Mn^{III}(terpy)\right]^{3+} + 5H_2O \quad (1)$$

The $[Mn_4{}^{IV}O_5(terpy)_4(H_2O)_2]^{6+}$ species formed in solution showed a lower concentration than that of the $[Mn_2^{IV,IV}O_2(terpy)_2(H_2O)_2]^{4+}$ species, so the voltammogram obtained (see Fig. 2) indicated only the redox process ascribed to the species of greater concentration. The complex $[Mn_4{}^{IV}O_5(terpy)_4(H_2O)_2]^{6+}$ formed in aqueous solution is compatible with dimers present in the photosynthesis II system; however, it is not capable of bringing about the oxidation of water. Therefore, the species formed in aqueous solution from the $[Mn_2^{III,IV}O_2(terpy)_2(H_2O)_2]^{3+}$ complex cannot act like homogeneous electrocatalysts for the

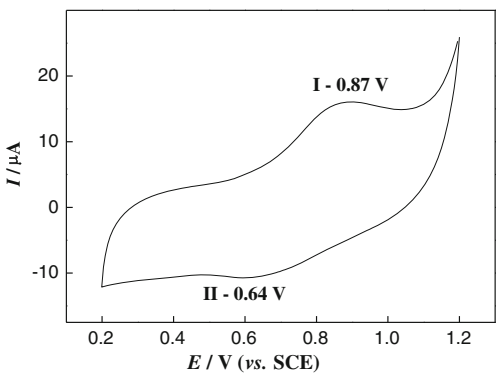

Fig. 2 Cyclic voltammogram for 1.0 mmolL^{-1} of the $[Mn_2^{IV,IV}O_2(terpy)_2(H_2O)_2]^{4+}$ complex in 0.5 molL^{-1} $NaNO_3$ solution (pH = 4.7) from 0.2 to 1.2 V vs. SCE potential range at 25 mVs^{-1}

oxidation of water [20]. The formation of the new μ-oxo-bridged occurs to stabilize the cluster structure in aqueous solution [20, 21].

Recently, our research group has conducted studies on the electrochemical behavior of the $[Mn_4{}^{IV}O_5(terpy)_4(H_2O)_2]^{6+}$ complex in solution [22]. Due to possibility of dimerization of the manganese complexes, it was possible form a polymer film on the substrate of ITO and glassy carbon electrode, where the mechanism of the formation can be explained by the rearrangement of the bonds made during oxidation of Mn^{III} (high spin) to Mn^{IV}, which are relatively rapid in the time of the potential scan applied. Due to the rearrangement of the orbitals $dx^2–y^2$ and pπ for the formation of the new μ-oxo bond, a greater stability is provided for the polymer complex containing a Mn^{IV} ion.

During the reduction of the metal cation of the $[Mn_2{}^{IV,IV}O_2(terpy)_2(H_2O)_2]^{4+}$ complex, one or two aqua ligands can be substituted by the anions of the supporting electrolyte; however, manganese centers are maintained in the structure of the complex [20]. Thus, it is important that the anions present in the supporting electrolyte be weaker in the spectrochemical series in relation to the aqua ligand in the coordination of the manganese ions in the complex. The supporting electrolytes $NaNO_3$ and Na_2SO_4 do not affect the stability of the complex in non-buffered aqueous solution [2, 20]. The cyclic voltammetry studies demonstrate that the manganese complex containing terpyridine as ligand shows a greater stability in aqueous solution, when compared to the complexes containing other ligands, such as 2,2-bipyridine (bpy) and phenanthroline (phen), in accordance with the results found in the literature [1, 2, 20, 21].

The electrochemical behavior of the complex $[Mn_2{}^{IV,IV}O_2(terpy)_2(H_2O)_2]^{4+}$ as a function of pH (2.8–9.8) was studied by cyclic voltammetry for a scan rate of 25 mVs^{-1}. Two linear regions were observed for the redox potential ($E_{1/2}$) of the complex with variation in pH, one for acid medium (pH 2.8 to 5.8) and another for basic medium (pH 6.8 to 9.8), with an intersection point at pH 6.0. For pH values lower than 5.8, the redox potential of the complex shifted to more positive potentials. The magnitude of the redox potential was linear with variation of the pH, with a slope of approximately −132 $mVpH^{-1}$. The coefficient observed indicates a process controlled by the loss of two protons per electron, in agreement with Eq. 1.

For the second response region, the potential values increased with pH. A linear correlation of the potential magnitude with variation of the pH, with a slope of approximately +96 $mVpH^{-1}$, was observed in the pH range of 5.8 to 9.8, indicating that in basic medium the process is also controlled by the loss of two protons per electron. However, in this pH range, the formation of other sub-species of manganese can be observed (Eq. 2):

$$2\left[Mn_2^{III,IV}O_2(terpy)_2(H_2O)_2\right]^{3+} + H_2O \rightleftharpoons \left[Mn_2^{III,III}O_2(terpy)_2(H_2O)_2\right]^{2+} + [Mn^{IV}O_2] + \left[Mn^{IV}O(terpy)(H_2O)_2\right]^{2+} + terpy + 2H^+ \quad (2)$$

At pH higher than 9.8, no redox process of the complex was observed. This behavior is probably due to an elevated formation of a mixed complex and/or generation of manganese oxide with hydroxyl ions of the solution, making it electroinactive.

Hydrodynamic Characterization by Linear Sweep Voltammetry with a Rotating Disk Electrode

For the $[Mn_2{}^{IV,IV}O_2(terpy)_2(H_2O)_2]^{4+}$ complex, stability is ascribed to the rapid evolution toward tetranuclear species. This phenomenon can be demonstrated by the type of ligand, where for the formation of $[Mn_2{}^{IV,IV}O_2(L)_4]^{4+}$ with binuclear ligands such as 2,2-bipyridine and 1,10-phenanthroline, it is necessary to have a lost coordination of a ligand and formation of two new μ-oxo-bridges. Unlike in what occurs in the formation of the $[Mn_2{}^{IV,IV}O_2(terpy)_2(H_2O)_2]^{4+}$ species, where there is no lost coordination of the terpyridine ligand on the manganese ion, and consequently, the formation of the complex is due to a single μ-oxo-bridged between two binuclear molecules. This behavior can be facilitated by the presence of aqua ligands in the structure, which leads to the formation of the new μ-oxo-bridged, occurring during the reduction/oxidation process of the manganese centers of the complex. Therefore, a hydrodynamic electrochemical study was carried out, utilizing a rotating disk electrode, in order to determine important kinetic parameters that help in the study of the stability and electrochemical behavior of the $[Mn_2{}^{IV,IV}O_2(terpy)^2(H_2O)_2]^{4+}$ complex in aqueous solution. Figure 3 shows the voltammetric profile of RDE for the complex in aqueous solution in the potential range of 0 to 1.0 V vs. SCE. The voltammograms in the RDE were performed in 0.5 $molL^{-1}$ $NaNO_3$ at a scan rate of 25 mVs^{-1}, varying the rotation of the electrode in the range of 100 to 5,000 rpm. The voltammetric profile demonstrates a kinetically irreversible process, which favors the reduction of the species in solution, observed by the cathode slope with varying rotation of the electrode. The same redox process was observed when the potential was applied in the anodic direction. The irreversibility of the system demonstrates that in aqueous solution the complex possesses greater stability in the redox pair $Mn^{IV}Mn^{IV}$, which is reduced irreversibly to $Mn^{III}Mn^{IV}$ along with disproportioning of the complex, forming subspecies of manganese (Eq. 1). The

irreversibility of system on RDE when compared to cyclic voltammetry can be ascribed to isovalence of the metallic nucleus. Due to the movement of convection, there is no adequate time for the reduced Mn^{IV} to Mn^{III} be oxidized to Mn^{IV}. Thus, only voltammetric waves on cathodic region were observed. Furthermore, the absence of Mn^{III} in the initial complex structure prevents the formation of the oxidation wave.

In irreversible systems, it is necessary to apply higher potentials than in reversible systems, in order to overcome the energy of activation and allow the occurrence of the oxi-reduction reaction of the complex on the surface of the electrode. Thus, the electron transfer rate constant (k_e) for an irreversible system increases with the potential applied on the electrode until reaching the level of the current limit [23]. In irreversible systems, there is no equilibrium of the species on the surface, and consequently, the Nernst equation for redox potentials as a function of the electrode rotation rate is not applicable. This is due to the fact that the half-wave potential ($E_{1/2}$) is dependent on the mass transfer coefficient (k_d) [23]. k_d describes the diffusion rate in the double layer, which is controlled by the variation in the forced convection (rotation). For an irreversible system, the magnitude of the standard electron transfer rate constant (k_0) is very much less than the mass transfer coefficient k_d ($k_0 << k_d$).

Based on RDE curves of the oxo–manganese complex reduction (Fig. 3) linearity of the $\log(I_L - I/I)$ vs. $E_{applied}$ (V) was observed by equation of Heyrovský-Ilkovic for an irreversible system:

$$E_{aplicado} = E_{1/2}^{irr} - \frac{2.303RT}{\alpha_c nF} \log \frac{I_L - I}{I} \quad (3)$$

where α_c is the cathodic charge transfer coefficient, I the current observed, I_L the limiting current for a fixed potential (0.1 V *vs.* SCE), and $E_{1/2}$ the half-wave potential. As a consequence, the values of the cathodic charge transfer coefficient and half-wave potential were determined by the slope of the straight line:

$$slope = \frac{2.303RT}{\alpha_c nF} \quad (4)$$

The values $\alpha_c n$ and $E_{1/2}$ for each rotation studied are shown in Table 1. It was shown that the magnitude of the electron transfer coefficient is influenced by the electrode rotation rate. While the half-wave potential of the reduction of the complex in aqueous medium moves toward cathodic potentials and becomes constant for rotation higher than 1,500 rpm (157.08 rad s^{-1}). The data can be analyzed based on the kinetics of the reaction, where the observed current (I), for a given potential, is related to the electrode rotation rate (ω) through the Koutecky-Levich equation [23, 24]:

$$\frac{1}{I} = \frac{1}{I_k} + \frac{1}{I_L} \quad (5)$$

where I_k represents the kinetic current (lack of any effect of mass transport) and I_L the limiting diffusion current, which is related to the electrode rotation rate (ω) by the Levich equation [23, 24]:

$$I_L = 0.62nFAC_oD^{2/3}n^{-1/6}\omega^{1/2} \quad (6)$$

where A is the area of the electrode (0.071 cm^2), D the diffusion coefficient ($cm^2 s^{-1}$), ω the electrode rotation rate (rad s^{-1}), ν the kinetic viscosity of the solvent (9.025×10^{-3} $cm^2 s^{-1}$), C_o the concentration of the complex in solution, F the Faraday constant (96,485.3 C mol^{-1}), and n the number of electrons involved in the reaction transfer.

Selecting the potential range between the level of the limiting current and the linear region close to the half-wave potential (Tafel region), a plot was constructed of I^{-1}

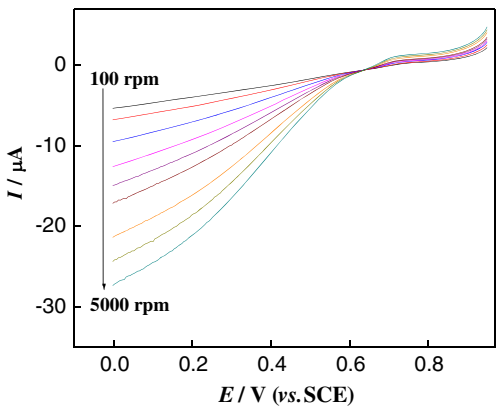

Fig. 3 Linear sweep voltammogram for 1.0 mmol L^{-1} of the $[Mn_2^{IV,IV}O_2(terpy)_2(H_2O)_2]^{4+}$ complex in 0.5 mol L^{-1} $NaNO_3$ solution at 100, 200, 500, 1,000, 1,500, 2,000, 3,000, 4,000, and 5,000 rpm. v=25 mV s^{-1}

Table 1 Values of $\alpha_c n$ and $E_{1/2}$ obtained from Heyrovský-Ilkovic equation (Eq. 3)

Rotation/rad s^{-1}	Slope	$\alpha_c n$	$E_{1/2}$/mV	r values
10.472	0.3092	0.191	418	0.998
20.944	0.2998	0.197	406	0.999
52.360	0.2807	0.210	391	0.999
104.720	0.2706	0.218	380	0.999
157.080	0.2659	0.220	376	0.999
209.440	0.2570	0.230	375	0.999
314.159	0.2481	0.238	375	0.999
418.879	0.2457	0.241	375	0.999
523.599	0.2452	0.251	375	0.999

as a function of $\omega^{-1/2}$ (Koutecky-Levich plot). Based on the linear coefficient of the relation I^{-1} vs. $\omega^{-1/2}$, kinetic current (I_k) values were obtained (see Table 2), which can be represented by Eq. 7:

$$I_k = nFAk_e^{'}C \tag{7}$$

Considering that the system shows only oxidized species in the middle of the solution, that is, where there is at least electrochemical reduction, we have the relation:

$$k_e^{'} = k_0 \exp\left[-\alpha_c nF\left(E - E^{\theta}\right)/RT\right] \tag{8}$$
$$\log k_e^{'} = \log k_0 - \frac{\alpha_c nF}{2.303RT}E$$

where k_o is the standard electron transfer rate constant. Thus, applying *log* k_e' as a function of the potential applied gives the value of k_o and $\alpha_c n$ by the linear coefficient and slope, respectively. The standard electron transfer rate constant for reduction of the complex on the surface of the electrode was $5.76\times10^{3}\,s^{-1}$. Due to the lack of equilibrium of the species on the electrode surface, the variation in the electron transfer coefficient was observed depending on the potential applied, according to the Heyrovský-Ilkovic equation (Eq. 3). However, using Eq. 8, it was possible to obtain a single value for the cathodic charge transfer coefficient of 0.71, confirming that the system was irreversible.

The Levich equation (Eq. 6) was used to calculate the diffusion coefficient of the complex in aqueous solution utilizing the limiting current values (0.1 V vs. SCE) for different electrode rotation rates. The Levich plot showed linearity of the limiting current with $\omega^{1/2}$, according to Eq. 9:

$$I_L(A) = 7.61\times10^{-7} + 1.03 \tag{9}$$
$$\times10^{-6}\omega^{1/2}\left(A\ \mathrm{rad}^{1/2}\mathrm{s}^{-1/2}\right)\ r = 0.9989$$

According to Levich equation, the diffusion coefficient for the reduction of the complex in aqueous solution of $1.16\times10^{-6}\,cm^2\,s^{-1}$ was calculated.

Table 2 Kinetic current values and rate constant of apparent electronic transfer obtained from Koutecky-Levich equation (Eqs. 5 and 7)

E/mV	I_k/A	k_e'/s^{-1}
450	1.74×10^{-4}	2.58×10^{-2}
490	4.45×10^{-5}	6.58×10^{-3}
550	1.01×10^{-5}	1.49×10^{-3}
570	4.92×10^{-6}	7.28×10^{-4}
590	3.73×10^{-6}	5.52×10^{-4}

Electrochemical Behavior of the Glassy Carbon Electrode Modified with a Complex of Oxo–Manganese–Terpyridine Immobilized on Nafion® (GC-Nafion/MnTerpy)

After the formation of the Nafion® film and immobilization of the complex $[Mn_2{}^{IV,IV}O_2(terpy)_2(H_2O)_2]^{4+}$ on the electrode surface, the electrochemical behavior of the modified electrode (GC-Nafion/MnTerpy) was investigated by cyclic voltammetry in a solution of 0.5 $mol\,L^{-1}$ $NaNO_3$ (pH 4.7). Figure 4 shows the typical cyclic voltammogram with an anodic peak at 0.85 V vs. SCE and cathodic peak at 0.60 V vs. SCE for the modified electrode at a scan rate of 25 mV s^{-1}. Peaks I and II can be ascribed to the redox couple $Mn^{IV}Mn^{IV}/Mn^{III}Mn^{IV}$. The redox potentials for the modified electrode are very close to the values obtained for the complex studied in aqueous solution, indicating that immobilization of the electroactive species on the ion-exchange polymer film did not alter the structure and/or did not affect the electrochemical properties of the complex.

Through the redox process shown by the modified electrode, study of scan rate was carried out. The dependence of the peak current (anodic—I_{pa} and cathodic—I_{pc}) demonstrated a linear relation for low scan rate, while at high scan rate (≥75 $mV\,s^{-1}$), the peak current was shown to be linear with the square root of the scan rate. This behavior indicates that the modified electrode is controlled by two systems, where for low scan rate, the redox process is controlled by the surface mechanism, while for high scan rate the process is controlled by diffusion.

The concentration of electroactive species was calculated from the slope of the linear relation of peak current as a function of the scan rate, as represented by Eq. 10 [24]:

$$I_p = \frac{n^2F^2A}{4RT}v \tag{10}$$

where I_p is the peak current (A), n the number of electrons, F the Faraday constant ($C\,mol^{-1}$), A the area of the electrode

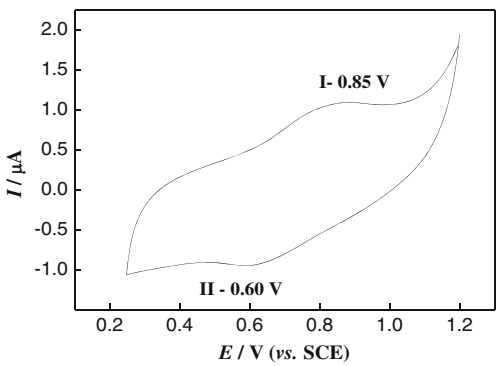

Fig. 4 Cyclic voltammogram of the GC-Nafion/MnTerpy modified electrode in 0.5 $mol\,L^{-1}$ $NaNO_3$ solution (pH = 4.7). v=25 $mV\,s^{-1}$

surface (0.071 cm^2), Γ the concentration of electroactive species ($molcm^{-2}$), R the gas constant ($CK^{-1}mol^{-1}$), T the temperature (K), and v the scan rate (Vs^{-1}). Using the relation of peak current as a function of the scan rate (<50 mVs^{-1}), it was possible to obtain the concentration of electroactive species (Γ) on the electrode surface, i.e., $2.83\times10^{-10}molcm^{-2}$. The voltammograms demonstrate a displacement of the peak to more positive potentials with variation in the scan rate, the separation of the anodic (E_{pa}), and cathodic (E_{pc}) peak potentials was about 250 mV, indicating a quasi-reversible process.

The effect of the counter-ion (anion) on the electrochemical behavior of the modified electrode was determined utilizing solution of NaCl, $NaNO_3$, $NaClO_4$, and Na_2SO_4 at 0.5 mol L^{-1}. The redox potential of the modified electrode in electrolyte solution containing the different anions changed to more cathodic values with the increase in ionic radium of the anion, demonstrating that the counter ions influence the voltammetric behavior of the modified electrode. The redox potential was linearly dependent on the ratio [ion charge]/[ionic radium], indicating the insertion of the ion in the polymer matrix (Fig. 5). This behavior suggests the mobility of the supporting electrolyte ions necessary to maintain electroneutrality on the electrode surface during the redox process. The main factors that influence the permeability of the counter ion in the polymer film containing the complex are: (1) the radium of the hydrated ion, (2) the radium of the ion channel in the polymer film, and (3) the interaction between ion and complex in the charge counterbalance, influencing electrostatic interactions and ionic polarities. A similar behavior has been observed in modified electrodes with the metal hexacyanoferrate complex [25, 26] and polymer membrane [27]. Scholz and coworkers [28] have treated theoretically the electrochemical insertion of metal hexacyanoferrate ion based on experimental data:

$$E \approx cte + \frac{\phi}{zF}\frac{b}{r} \qquad (11)$$

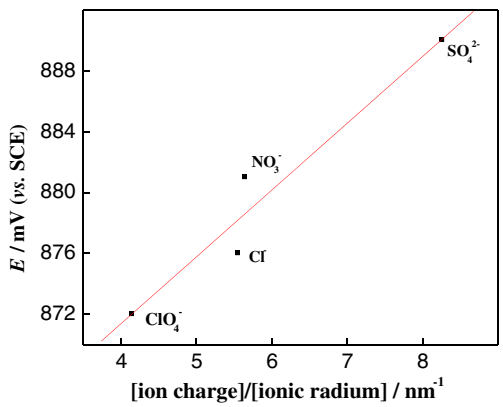

Fig. 5 Dependence of anodic potential in function of [ion charge]/[ionic radium] of the anions present on support electrolyte

where E is the potential of the electrode, b the charge of the ion of insertion, r the ionic radium of the ion, and ϕ the energy of insertion reaction for the Born model. The modified electrode showed a lower peak potential in the solution containing perchlorate ions, as in other studies performed in 0.5 $molL^{-1}$ $NaClO_4$. A study on the influence of the cation in the redox process has been carried out, but no change in redox potential and/or change in voltammetric profile were observed. Therefore, we can conclude that the effect of the counter ion is directly related to the immobilized complex, since the Nafion® membrane shows anionic properties.

Influence of the Concentration of the Nafion® Film

The study of the influence of the concentration of the ion-exchange polymer solution on the electrochemical behavior of the modified electrode was carried out by cyclic voltammetry. The solutions of Nafion® utilized for the formation of the film were 1, 2, 3, and 5 % *v*/*v* in ethanol of high purity. Based on the voltammograms obtained for the modified electrodes with different percentages of polytetrafluoroethylene sulfonate polymer, it was observed that the anodic peak potential of the modified electrode changed to more positive values. This behavior occurs due to the increase in electrical resistance on the surface of the electrode caused by the increase in the thickness of the polymer film [29]. A more detailed study of the influence of the quantity of polymer on the potential of the modified electrode was carried out by the variation in potential scan rate. The electrodes coated with 3 and 5 % *v*/*v* of the polymer solution showed two processes (adsorptive and diffusional) in the control of the magnitude of the current. However, for the electrodes coated with polymer films of low percentage (<3 % *v*/*v*), the peak currents were linear with scan rate in all cases studied. The different processes observed with the peak potentials indicate that the electrochemical behavior of the modified electrode is dependent on the composition of the polymer film on the surface of the electrode. Considering the results presented, the 2 % *v*/*v* solution of polytetrafluoroethylene sulfonate polymer was utilized for further studies.

The study of the influence of the volume of polymer solution deposited on the surface of the electrode on electrochemical behavior was carried out with aliquots of 3 to 9 μL of Nafion® (2 % *v*/*v*). The voltammograms were obtained in 0.5 $molL^{-1}$ $NaClO_4$ as supporting electrolyte (pH = 5.2), with scan rate of 25 mVs^{-1}, using a potential range of 0.45 to 1.2 V vs. SCE. The peak current (I_{pa} and I_{pc}) as a function of the aliquot of the polymer on the surface of the electrode indicates greater peak redox current for the modified electrode with 3 μL of polymer solution (see Table 3). This behavior can be ascribed to a greater dispersion of the polymer film on the electrode surface, as well as achieving a thin film.

Table 3 Peak current values in function of aliquot of the Nafion® 2 % *v/v*

Nafion® volume/μL	Anodic peak current/A	Cathodic peak current/A
3	1.74×10^{-6}	-1.76×10^{-6}
5	1.23×10^{-6}	-1.05×10^{-6}
7	9.01×10^{-7}	-8.33×10^{-7}
9	9.79×10^{-7}	-8.57×10^{-7}

Effect of pH

The effect of pH was investigated utilizing 0.1 $molL^{-1}$ acetate buffer containing 0.5 $molL^{-1}$ $NaClO_4$ in the pH range of 2 to 8. The cyclic voltammograms obtained at pH over 6.0 and below pH 3.0 did not show any redox process, which can be ascribed to a decomposition of the complex in the polymer film. For very acid pH, the polymer film is affected by the concentration of hydronium ions (H_3O^+) in the medium, able to cause ion exchange with the immobilized complex at the active sites of polytetrafluoroethylene sulfonate [30]. However, for a pH range between 3.0 and 5.2, the modified electrode showed better stability, indicating that the glassy carbon electrode modified with the oxo–manganese–terpyridine complex immobilized in 2 % *v/v* polytetrafluoroethylene sulfonate can be applied in this pH range without loss of electrochemical activity.

Study of the Electrochemical Activity of the Electrode Modified for Oxidation of Dopamine

The GC-Nafion/MnTerpy modified electrode was applied as a sensor for dopamine (DA). The voltammetric measurements were made in an electrochemical cell with 20 mL of 0.5 $molL^{-1}$ $NaNO_3$ as the supporting electrolyte, applying a scan rate of 25 mVs^{-1} in a potential range of 0.45 to 1.2 V vs. SCE at different concentrations of DA. The mechanism of the modified electrode in the presence of dopamine was based on two redox reactions, where the first reaction involves the chemical reduction of Mn^{IV} by DA, forming Mn^{III} on the surface of the electrode and *o*-quinone in solution. The Mn^{III} ion generated is then oxidized electrochemically to Mn^{IV}. In the presence of dopamine, an increase in the anodic peak current at a potential of 0.87 V vs. SCE can be observed as a function of the DA concentration in solution (Supplementary Data). In the presence of 0.556 $mmolL^{-1}$ dopamine, the anodic peak current obtained with the modified electrode was three times greater than that obtained with the same electrode in the absence of DA. The good stability of the complex could be ascribed to the efficient immobilization of the complex by the Nafion® membrane. On the other hand, an anodic redox peak of approximately 1.0 V vs. SCE is observed for DA concentrations over 0.338 $mmolL^{-1}$, which could be ascribed to the oxidation of *o*-quinone to aminochrome without electron mediation of the complex immobilized on the surface electrode.

The effect of scan rates (5 to 200 mVs^{-1}) on the voltammetric response of the electrode modified in the presence of 0.556 $mmolL^{-1}$ DA was investigated. A linear dependence of the anodic peak current on the square root of the scan rate was observed, indicating that the process was diffusional for the reduction of Mn^{IV} by DA on the surface of the electrode. However, for scan rates over 100 mVs^{-1}, a loss of the redox process was observed, where it could have been ascribed to the slow kinetics of electron transfer of the electrode modified for DA. Therefore, a kinetic study by the Tafel region in the presence of DA was performed to elucidate the kinetics of electron transfer between the metal center of the complex immobilized on the polymer membrane and the analyte. The Tafel region represents the kinetics of electron transfer between DA and the metal centers of the complex. In this context, the electron transfer coefficient as a function of the number of electrons involved in the determinant step of the redox process can be obtained by the slope (Eq. 4) of the Tafel relation (log *I* vs. *E*; see Fig. 6). The variation in the electron transfer coefficient of 0.10 to 0.08 was observed with increase in DA concentration (0.012 to 0.556 $molL^{-1}$), demonstrating a response mechanism of slow rate of electron transfer and dependent on DA concentration.

The apparent order of reaction (*q*) for the respective concentrations of dopamine was determined by the Tafel region with potential fixed based on the linear relation of log *I* versus log concentration of DA, where the apparent order of reaction varied from 0.36 to 0.32 in relation potential range of the Tafel region (0.79 to 0.86 V vs. SCE). Therefore, *q* is dependent on the

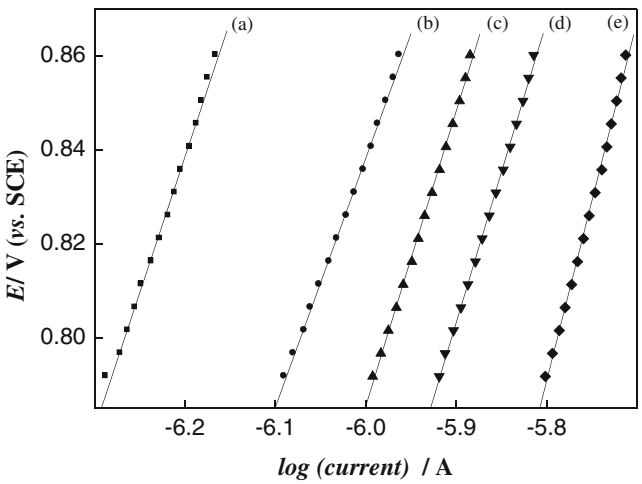

Fig. 6 A Tafel relation for modified electrode in presence of *a* 0.012, *b* 0.148, *c* 0.244, *d* 0.431, and *e* 0.556 $mmolL^{-1}$ of dopamine

concentration of DA at an applied potential, where it is defined by:

$$q = \left(\frac{d\log I}{d\log[DA]}\right)_{E,T} \quad (12)$$

The cyclic voltammograms obtained for the modified electrode in the presence of DA showed an increase in current with the addition of DA at a concentration higher than 0.025 mmol L^{-1}, demonstrating electrocatalysis of DA oxidation by the metal centers of the complex. The analytical curve was obtained with addition of 50 to 1,200 μL of DA, resulting in a linear equation of I (μA)=1.07+3.83[dopamine (mmolL^{-1})]. The analytical curve displayed linearity in the concentration range of 0.025 to 0.556 mmolL^{-1}, with a limit of detection of 0.020 mmolL^{-1}.

The influence of possible interferences with potential in the voltammetric response of the modified electrode was investigated. The voltammetric measurements were made in 0.5 mol L^{-1} $NaClO_4$ (pH 7.0) containing 1.0 mmolL^{-1} citric acid, tartaric acid, oxalic acid, acetylsalicylic acid, caffeine, saccharin, fructose, glucose, and saccharose. None of the substances tested showed interference with the response of the modified electrode, which could have been due to the presence of Nafion® on the surface of the electrode, as it is negatively charged by sulfonic groups and capable of increasing the adsorption of DA on the surface of the electrode and repelling anions present in the solution, this being in accordance with the data found in the literature [5, 19].

Conclusion

The complex $[Mn_2^{IV,IV}O_2(terpy)_2(H_2O)_2]^{4+}$ demonstrated kinetically irreversible redox processes, observed by studies of linear sweep voltammetry with a rotating disk electrode. Therefore, the greater stability in solution was ascribed to the rapid evolution for tetranuclear complexes by the process of dimerization, which was confirmed by studying the effect of pH. For the modified electrode, the film of Nafion® was promising in the immobilization by ion exchange with the complex $[Mn_2^{IV,IV}O_2(terpy)_2(H_2O)_2]^{4+}$. Thus, the modified electrode showed good stability in aqueous solution in the pH range of 3.0 to 5.0. Where, the better voltammetric measurements were obtained under the following conditions: potential range of 0.45 to 1.2 V vs. SCE, utilizing 0.5 molL^{-1} $NaClO_4$ as the supporting electrolyte (pH = 5.2) with scan rate of 25 mVs^{-1}. The electrochemical response of the glassy carbon electrode modified with the oxo–manganese–terpyridine complex showed dependence on the concentration of DA with a slow rate of electron transfer (0.020 molL^{-1} detection limit). The apparent order of the reaction was obtained in the range of 0.36 to 0.32 in relation to the Tafel region (0.79 to 0.86 V vs. SCE) present with the different additions of dopamine (0.012 to 0.556 molL^{-1}).

Acknowledgments The authors are grateful to FAPESP for the Scientific Initiation Fellowship awarded to C. S Martin (2009/11079-1) and CNPq for research support (481827/2007-2). SJT is also thanked. Dr. A. Leyva helped with English translation and editing of the manuscript.

References

1. T. Tzedakis, Electrochim. Acta **46**, 99–109 (2000)
2. M.N. Collomb, A. Deronzier, A. Richardot, J. Pecaut, New J. Chem. **23**, 351–353 (1999)
3. V.L. Pecoraro, *Manganese redox enzymes* (VCH, New York, 1992)
4. D. Srinivas, S. Sivasanker, Catal. Surv. Asia **7**, 121–132 (2003)
5. K. Ozette, P. Battioni, P. Leduc, J.F. Bartoli, D. Mansuy, Inorg. Chim. Acta **272**, 4–6 (1998)
6. N.W.J. Kamp, J.R.L. Smith, J. Mol. Catal. A: Chem. **113**, 131–145 (1996)
7. R. Ganesan, B. Viswanathan, J. Mol. Catal. A: Chem. **223**, 21–29 (2004)
8. T. Tzedakis, Y. Benzada, M. Comtat, Ind. Eng. Chem. Res. **40**, 3435–3444 (2001)
9. J.J. Dannacher, J. Mol. Catal. A: Chem **251**, 159–176 (2006)
10. R. Manchanda, G.W. Brudvig, R.H. Crabtree, Coord. Chem. Rev. **144**, 1–38 (1995)
11. W. Ruttinger, G.C. Dismukes, Chem. Rev. **97**, 1–24 (1997)
12. M.C. Ghosh, J.W. Reed, R.N. Bose, E.S. Gould, Inorg. Chem. **33**, 73–78 (1994)
13. M.N.C. DunandSauthier, A. Deronzier, X. Pradon, J. Am. Chem. Soc. **119**, 3173–3174 (1997)
14. S.R. Cooper, M. Calvin, J. Am. Chem. Soc. **99**, 6623–6630 (1977)
15. D.R. Gamelin, M.L. Kirk, T.L. Stemmler, S. Pal, W.H. Armstrong, J.E. Pennerhahn, E.I. Solomon, J. Am. Chem. Soc. **116**, 2392–2399 (1994)
16. H.Y. Chen, R. Tagore, S. Das, C. Incarvito, J.W. Faller, R.H. Crabtree, G.W. Brudvig, Inorg. Chem. **44**, 7661–7670 (2005)
17. S.R. Cooper, G.C. Dismukes, M.P. Klein, M. Calvin, J. Am. Chem. Soc. **100**, 7248–7252 (1978)
18. M. Suzuki, S. Tokura, M. Suhara, A. Uehara, Chem. Lett. **477–480** (1988)
19. C. Baffert, H.G. Chen, R.H. Crabtree, G.W. Brudvig, M.N. Collomb, J. Electroanal. Chem. **506**, 99–105 (2001)
20. C. Baffert, S. Romain, A. Richardot, J.C. Lepretre, B. Lefebvre, A. Deronzier, M.N. Collomb, J. Am. Chem. Soc. **127**, 13694–13704 (2005)
21. H.Y. Chen, J.W. Faller, R.H. Crabtree, G.W. Brudvig, J. Am. Chem. Soc. **126**, 7345–7349 (2004)
22. C.S. Martin, M.F.S. Teixeira, Dalton Trans. **40**, 7133–7136 (2011)
23. C.M.A. Brett, A.M.O. Brett, *Electrochemistry: principles, methods, and applications,* (Oxford University Press, Oxford, 1993)
24. A.J. Bard, L.R. Faulkner, *Electrochemical methods: fundamentals and applications*, 2nd edn. (Wiley, New York, 2001)
25. M.F.S. Teixeira, A. Segnini, F.C. Moraes, L.H. Marcolino, O. Fatibello, E.T.G. Cavalheiro, J. Braz. Chem. Soc. **14**, 316–321 (2003)
26. P. Wu, C.X. Cai, J. Solid State Electrochem. **8**, 538–543 (2004)
27. T.R.L. Dadamos, M.F.S. Teixeira, Electrochim. Acta **54**, 4552–4558 (2009)
28. M.B. Soto, F. Scholz, J. Electroanal. Chem. **521**, 183–189 (2002)
29. S.H. Chen, R. Yuan, Y.Q. Chai, L.G. Min, W.J. Li, Y. Xu, Electrochim. Acta **54**, 7242–7247 (2009)
30. M.M. Nasef, A.H. Yahaya, Desalination **249**, 677–681 (2009)